ECOHYDROLOGY
Ecohydrol. **4**, 564–576 (2011)
Published online 22 June 2010 in Wiley Online Library
(wileyonlinelibrary.com) DOI: 10.1002/eco.132

Thermopeaking in Alpine streams: event characterization and time scales

Guido Zolezzi,[1]* Annunziato Siviglia,[1] Marco Toffolon,[1] and Bruno Maiolini[2]

[1] *Department of Civil and Environmental Engineering, University of Trento, Trento, Italy*
[2] *IASMA Research and Innovation Centre, Fondazione Edmund Mach, Environment and Natural Resources Area, Trento, Italy*

ABSTRACT

The present study provides a detailed quantification of the 'thermopeaking' phenomenon, which consists of sharp intermittent alterations of stream thermal regime associated with hydropeaking releases from hydroelectricity plants. The study refers to the Noce River (Northern Italy), a typical hydropower-regulated Alpine stream, where water stored in high-altitude reservoirs often has a different temperature compared with the receiving bodies. The analysis is based on a river water temperature dataset that has been continuously collected for 1 year at 30-min intervals in four different sections along the Noce River. A suitable threshold-based procedure is developed to quantify the main characteristics of thermopeaking, which is responsible for thermal alterations at different scales. The application of Wavelet Transform allows to separately investigate the thermal regime alterations at sub-daily, daily and weekly scales. Moreover, at a seasonal scale, patterns of 'warm' and 'cold' thermopeaking can be clearly detected and quantified. The study highlights the relevance of investigating a variety of short-term alterations at multiple time scales for a better quantitative understanding of the complexity that characterizes the river thermal regime. The outcomes of the analysis raise important interdisciplinary research questions concerning the effects of thermopeaking and of the related short- and medium-term effects on biological communities, which have been rather poorly investigated in ecological studies. Copyright © 2010 John Wiley & Sons, Ltd.

KEY WORDS thermopeaking; regulated Alpine rivers; river temperature; hydropower; Wavelet Transform

Received 29 October 2009; Accepted 14 March 2010

INTRODUCTION

In Alpine regions, hydroelectricity generation is increasingly becoming a key power source and its ability to quickly and inexpensively respond to short-term changes in demand make it the suitable tool for answering to the necessities of the deregulated energy market (Holland and Mansur, 2008). This economical need is reflected in the temporal patterns of dam operations with consequences for the water bodies that receive downstream releases in the form of 'hydropeaking' (e.g. Gore and Petts, 1989), typically consisting in sharp releases of water in the river reaches below dams. The unsteadiness related to this highly intermittent phenomenon has cascading effects on both the biotic (Rea and Ganf, 1994; Nilsson *et al*., 1997; Cereghino and Lavandier, 1998; Blanch *et al*., 1999; Jansson *et al*., 2000; Scruton *et al*., 2008; Bruno *et al*., 2009) and abiotic compartments (Foulger and Petts, 1984; Montgomery *et al*., 1999; Bunn and Arthington, 2002; Frutiger, 2004; Sawyer *et al*., 2009).

Hydropeaking may also significantly affect the thermal regime of rivers (Ward and Stanford, 1979). Indeed, especially in mountain areas, releases from high-elevation reservoirs are often characterized by a markedly different temperature from that of the receiving body, thus causing also sharp water temperature variations which can therefore be named 'thermopeaking'. Nowadays, understanding heat fluxes and thermal dynamics within rivers is increasingly becoming an issue of great relevance (Hannah *et al*., 2008). Anthropogenic influences and climate changes alter the thermal regime of rivers, which can lead to shifts in aquatic species composition and changes in the rates of biogeochemical processes (Caissie, 2006). A main issue is to detect the role of the several mechanisms that control river temperature at different temporal and spatial scales (e.g. Brown and Hannah, 2008; Burkholder *et al*., 2008). This is achieved by assessing the relative contributions of heat advection and diffusion processes as well as those of external sources located in the atmosphere and in the riverbed (Webb *et al*., 2008; Toffolon *et al*., 2009) and due to the input of natural and artificial lateral tributaries (Siviglia and Toro, 2009). Several studies have focused on thermal and ecological effects of hydropower plants (Ward and Stanford, 1979; Cereghino and Lavandier, 1998; Flodmark *et al*., 2004; Grubbs and Taylor, 2004). However, little is known about the role of short-term temperature fluctuations related to thermopeaking occurring in the river reach below dams, although this can be a major cause of riverine habitat degradation posing serious threats to aquatic communities. The study of Steel and Lange (2007) acknowledges the ecological relevance of short temporal scales. For this purpose, they employ Wavelet Transform in order to analyse thermal alteration at time scales ranging from 1 to 32 days on daily average river water temperature

* Correspondence to: Guido Zolezzi, Department of Civil and Environmental Engineering, University of Trento, Trento, Italy.
E-mail: guido.zolezzi@ing.unitn.it

Copyright © 2010 John Wiley & Sons, Ltd.

series in the Willamette River Basin (Oregon, USA), characterized by the presence of large multipurpose dams. Hydropeaking releases associated with power production also alter the smallest time scales at hourly intervals. Frutiger (2004) analyses a 30-min interval temperature dataset to investigate the thermal effects of hydropower releases in the Ticino River (Switzerland). He recognizes the number of temperature peaks per day, unnaturally forced by hydropower releases, as a major ecological threat.

The purpose of the present work is to provide a quantitative representation and description of the rapid stream temperature oscillations associated with hydropeaking and on their short- and medium-term effects (daily and sub-daily) on the river thermal dynamics. We specifically focus on identifying the impacted temporal scales in altered rivers, which is crucial information for defining remediation actions.

In order to achieve this objective we first devise a technique suitable to identify 'hydropeaking' as well as 'thermopeaking events'. The approach is based on defining threshold rates of change in terms of the water level series first derivative, and on the application of Wavelet Transform (WT) which is particularly suitable to detect relevant scales of variability in time series (Foufoula-Georgiou and Kumar, 1995; Torrence and Compo, 1998). WT is increasingly being employed in hydrology (Kumar and Foufola-Georgiou, 1993; Katul *et al*., 1998) and namely in the study of altered flow regimes (Zolezzi *et al*., 2009). The study is based on a high time-resolution dataset (30 min) collected in the Noce River, a typical Alpine river catchment impacted by multiple hydropower plants located at different elevations.

MATERIALS AND METHODS

Study area

The study was conducted along the Noce River (Figure 1), a fourth-order Alpine stream located in the Trento Province, North-Eastern Italy. The river has been the subject of interdisciplinary monitoring for several years with the aim of quantifying the effects of hydropower production on riverine ecology. The total river length is 105 km, and it drains a typical Alpine catchment with an area of 1370 km^2. River basin elevations range from the confluence with the Adige River (226 m asl), up to Mount Cevedale peak (3769 m asl) (Figure 1). Major tributaries are the Vermigliana, the Rabbies and the Novella creeks. The Noce River is a main tributary of the Adige River. Dominant bed surface grain size ranges from coarse gravel to cobble with coarse sand matrix.

In the Noce River basin, hydropower is generated by three plants fed by four artificial reservoirs closed by dams. For this study, we consider two different junctions located, respectively, in the middle and lower parts of the catchment. The first confluence is located 5 km downstream the village of Malé where the unimpacted Rabbies Creek (yearly mean discharge 3·3 m^3/s, basin area 142 km^2) flows into the Noce River. The second confluence is located in the lower basin, near the village of Mezzocorona, where water stored in Santa Giustina reservoir (capacity of 182 × 10^{6}m^3) first passes through the Mollaro reservoir (capacity of 2 × 10^{6}m^3), and then feeds the Mezzocorona power plant that releases a maximum discharge of 60 m^3/s into the Noce River. The reservoir of Santa Giustina is created by a 152·5 m high dam, with the head at 532·5 m asl, maximum and minimum

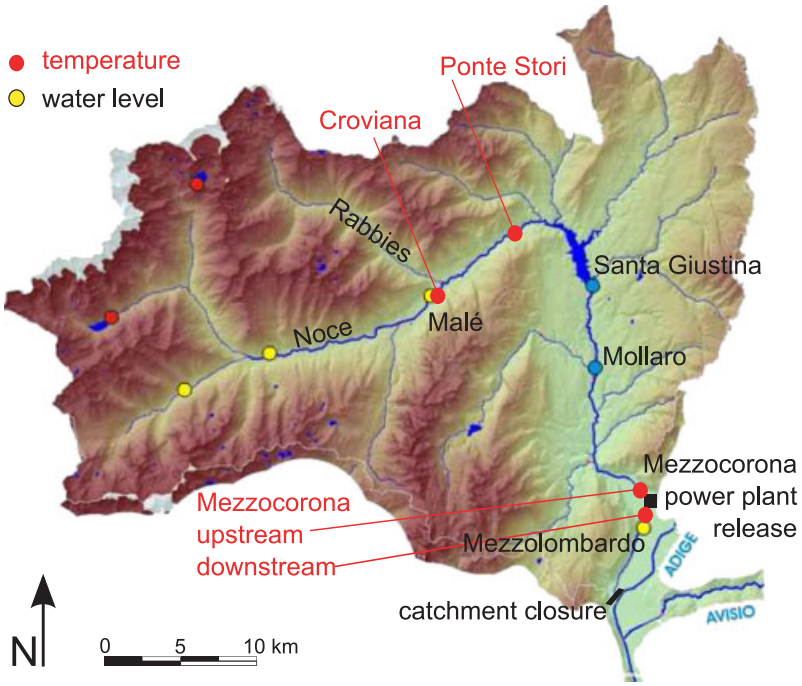

Figure 1. Study site: map of the Noce River catchment with location of the temperature and water level gauging stations (circles), where thermopeaking was investigated. The closure section of the catchment is located where the Noce River joins the main stem of the Adige River.

Copyright © 2010 John Wiley & Sons, Ltd.

DOI: 10.1002/eco

water levels at 530 and 445 m asl, respectively, and the hypolimnetic intake level at 437 m asl (Edison, 2008).

Data collection

Stream water temperature was monitored with high temporal and spatial resolution at four different locations along the basin through 10 StowAway TidbiT temperature dataloggers. The loggers have been placed along the main channel at suitable cross-sections up- and downstream of the two junctions. Namely, for the Rabbies junction, gauging sections were chosen near the village of Croviana (immediately upstream the confluence) and near the bridge named 'Ponte Stori' (Figure 1). Although the latter is located a few kilometres downstream the Rabbies-Noce confluence, no significant lateral tributary joins the Noce River in between. River water temperature was recorded at a sampling interval of 30 min beginning from 1st January until 31st December 2007. The loggers are waterproof, and detect temperatures ranging from −5 to +37 °C. The dataset is complemented by water level data available at three river sections (Figure 1): Noce River at Malé (upstream of Croviana), at Ponte Stori and a few hundreds of meters downstream the release of the Mezzocorona power plant. At these locations, a discharge-rating curve is also available.

Methods of data processing

Threshold analysis. In this section, we shortly describe a simplified procedure used for baseflow separation in order to precisely individuate the peaking events. This allows to estimate their main characteristics in terms of duration, intensity and time distribution. The procedure is based on establishing a threshold rate of change of the water level time series.

The first step is the preparation of the dataset, which in our case is the water level series on an annual basis. Streamflow data are obtained from water level data by means of a calibrated rating curve. Then, it is worth removing outlayers, if any, and applying a short-scale moving average (e.g. 1 h) in order to smooth high-frequency irregularities of the signal, often due to lack of instrumental precision. This allows to define the reference data $y(t)$ on which the events will be detected.

The second step is the individuation of the base flow (see Figure 2). The rate of change is given by the time derivative of the signal: $\dot{y} = \mathrm{d}y/\mathrm{d}t$. Its maximum values $\dot{y}_\mathrm{m} = \max\{|\dot{y}|\}$ allow to detect the initial and final times of a hydropeaking event when compared with a critical threshold that has to be chosen: $\dot{y}_\mathrm{c} = \dot{y}_\mathrm{m}/r_\mathrm{h}$. In the present analysis, we have chosen $r_\mathrm{h} = 3$, a threshold value that has been calibrated by manual analysis and that in general depends on the dataset. Afterwards, times t_ci for which $|\dot{y}| > \dot{y}_\mathrm{c}$ are selected, and the curve $y_\mathrm{c}(t)$ is reconstructed by joining the points $y(t_\mathrm{ci})$ through linear interpolation. Such a curve represents an approximation of the line separating the base flow $y_{\mathrm{b},0}(t)$ ($< y_\mathrm{c}$) from the peaks $y_\mathrm{p}(t)$ ($> y_\mathrm{c}$).

After that, short-term oscillations are removed from such approximation of the base flow by applying a moving average with a 1-day period in our case. This individuates the curve y_ba: as a second approximation only those points $y_{\mathrm{b},1}$ below such a curve ($y_{\mathrm{b},1}(t) < y_\mathrm{ba}(t)$) are selected. The definition of the base flow $y_{\mathrm{b},2}$ is further refined by excluding spikes close to the edges of peaking events, on the basis of absolute values of the centred differences referring to three subsequent values. The approximation of the base flow $y_{\mathrm{b},3}(t)$ is finally given by a linear interpolation of $y_{\mathrm{b},2}$ over the points removed from the original data series. Applying a moving average with a period of several days will allow to obtain a smooth signal.

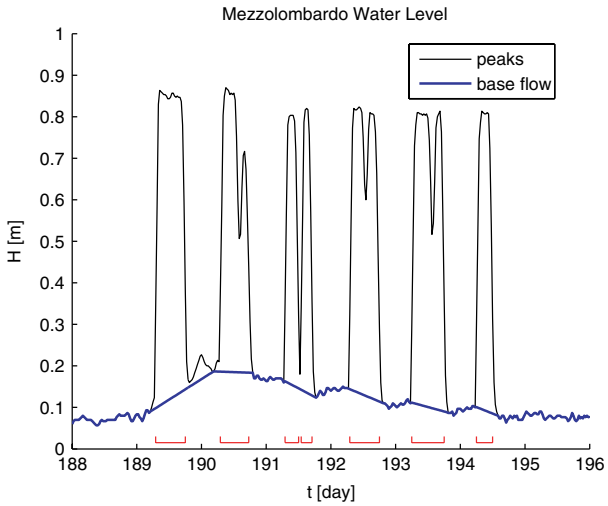

Figure 2. Water levels (black line) in Mezzolombardo from day 188 (Sunday, 8th July 2007) to day 195 (Sunday, 15th July 2007). The base flow (thick blue line) is identified through the procedure described in Section on Methods of Data Processing. The duration of the peaking events is visualized through the red segments close to the horizontal axis.

The third step is the individuation of the peaking events. The additional hydropeaks are defined as differences between the measured values and the base flow, i.e. $p(t) = y - y_{\mathrm{b},3}$, and negative values are excluded. Initial and closing times of each event are therefore easily determined as those separating periods of base flow ($p = 0$) from those with $p > 0$ that correspond to the hydropeaks. Once the peaks have been clearly recognized, the base flow can be redefined as the difference between the original data and the peak series, that is $y_\mathrm{b} = y - p$.

The fourth step is the recognition of multiple peaking events, defined by a significant reduction of the water level although higher than the base flow. We have defined that two events are separated if the signal drops below a reference level that is 20% of the peak value. This can indeed result from a temporary stop of at least one of the available turbine groups in the power plant. In general, the quantification of such threshold, therefore, depends on the characteristics of the hydropower system.

Finally, once the time series of the peaking events has been identified, it is straightforward to calculate the temporal length of each event, the height of the maximum peak value, and the time distribution during the year.

Copyright © 2010 John Wiley & Sons, Ltd.

DOI: 10.1002/eco

Wavelet Transform. WT has been applied to the recorded temperature series at the four locations near the Rabbies and the Mezzocorona junctions. It can be seen as a mathematical tool for extracting the dominant modes of variability from statistically non-stationary signals. In fact, WT is localized in time, and thus makes possible to detect time variations in the modes of variability associated to signal unsteadiness (see, e.g. Daubechies, 1992; Lau and Weng, 1995; Torrence and Compo, 1998). This is accomplished by letting the width of the wavelet to increase with the period, thus allowing a more efficient and accurate localization of changes in the dominant modes of variability with respect to the Windowed Fourier Transform (WFT), which uses a fixed-width window (Kaiser, 1994; Lau and Weng, 1995).

The continuous WT $W_n(s)$ of a discrete sequence x_n, $n = 1, 2, \ldots N$, at a given time scale s is defined as follows (Torrence and Compo, 1998):

$$W_n(s) = \sum_{n=0}^{N-1} x_{n'} \Psi^* \left(\frac{\eta}{s}\right) \tag{1}$$

where N is the length of the series, $\eta = (n' - n)\Delta t$ is the dimensionless time, Δt is the sampling time step, and superscript * indicates the complex conjugate.

The wavelet function $\Psi(\eta) = (2\pi s/\Delta t)^{1/2}\psi_0(\eta)$ is obtained by normalizing a 'mother' wavelet $\psi_0(\eta)$ such as to respect the following condition:

$$\sum_{k=0}^{N-1} |\Psi(s\ \omega_k)|^2 = N \tag{2}$$

for $k > N/2$, at each scale s. In Equation (2), $\omega_k = 2\pi k/(N\Delta t)$, for $k \leq N/2$, and $\omega_k = -2\pi k/N\Delta t$, otherwise. In addition, the mother wavelet should have unit energy, i.e $\int_{-\infty}^{\infty} |\psi_0(\omega')|\mathrm{d}\omega' = 1$. In this paper, we utilize the Morlet function as mother wavelet because it has been shown suitable to detect oscillating patterns (Torrence and Compo, 1998). It reads:

$$\psi_0(\eta) = \pi^{-1/4} \mathrm{e}^{i\omega_0\eta} \mathrm{e}^{-\eta^2/2} \tag{3}$$

with $\omega_0 = 6$.

The WT (1) is typically computed at the following set of scales:

$$s_j = s_0 2^{j\Delta j} \quad (j = 1, 2, \ldots, J) \tag{4}$$

where s_0 is the smallest scale considered in the analysis and $J = \Delta j^{-1} \log_2(N\Delta t/s_0)$, such that the largest scale is $N\Delta t$, i.e. the length of the time series. Furthermore, Δj is the inverse of the number of scales per each octave, and s_0 should be chosen such as to obtain a minimum Fourier period of $2\Delta t$. Because the equivalent Fourier period for the Morlet wavelet is given by $\lambda_j = 1{\cdot}03\ s_j$, in all computations we have chosen to use $s_0 = 2\Delta t$, and $\Delta j = 1/12$ such as to obtain a smooth wavelet spectrum.

The distribution of energy among the modes of variability (periods) is described by the Wavelet Power Spectrum (WPS) which is given by: $|W_n(s)|^2 = W_n(s)W_n^*(s)$. Interesting pieces of information on the nature of the signal can be obtained by analysing how signal energy, which is proportional to the amplitude of the fluctuations, varies with time. This can be obtained by computing the Scale-Averaged Wavelet Power (SAWPs) between the two scales of interest, $s_1 = s_0 2^{l_1\Delta j}$ and $s_2 = s_0 2^{l_2\Delta j}$, as follows:

$$\overline{W_n}^2 = \frac{\Delta j \Delta t}{C_\delta} \sum_{j=l_1}^{l_2} \frac{|W_n(s_j)|^2}{s_j} \tag{5}$$

where C_δ is a reconstruction factor, which for the Morlet wavelet with $\omega_0 = 6$ assumes the value 0·776. In addition, the time average of the WPS from $t_1 = n_1\Delta t$ to $t_2 = n_2\Delta t$ retains the most significant features of the time interval $[t_1, t_2]$:

$$\overline{W_p}^2(s) = \frac{1}{\Delta n} \sum_{n=n_1}^{n_2} |W_n(s)|^2 \tag{6}$$

where $\Delta n = n_2 - n_1$ and p is a suffix that identifies the time interval over which the average is computed. When the interval $[t_1, t_2]$ coincides with the length of the dataset, the quantity $\overline{W_p}^2$ represents the Global Wavelet Spectrum (GWS), an overall time-average measure of signal variability.

RESULTS

The results section is organized into four parts. First, we provide a quantitative characterization of the peaking events related with the Mezzocorona power plant by analysing the water level series, which is much more suitable with respect to the temperature series to detect events according to the procedure described in Section on Threshold Analysis. Second, having detected initial and final times of the hydropeaking events, it is straightforward to individuate thermopeaking on the temperature series. Third, we apply WT to the temperature series in order to point out the time scales at which thermopeaking affects the thermal regime of the Noce River reach under consideration. Finally, the analysis of the SAWP allows to investigate how the thermal alteration at each scale varies during the year.

Hydropeaking characterization

The main characteristics of hydropeaking events can be computed after applying the event-detection procedure described in Section on Threshold Analysis to separate the altered signal from the base flow.

We illustrate the phenomenon referring to the water level (H) series recorded downstream of the release from the Mezzocorona hydropower plant (Figure 1). The corresponding streamflow values are computed using a rating curve of the type

$$Q = a(b + H)^c \tag{7}$$

Copyright © 2010 John Wiley & Sons, Ltd.

DOI: 10.1002/eco

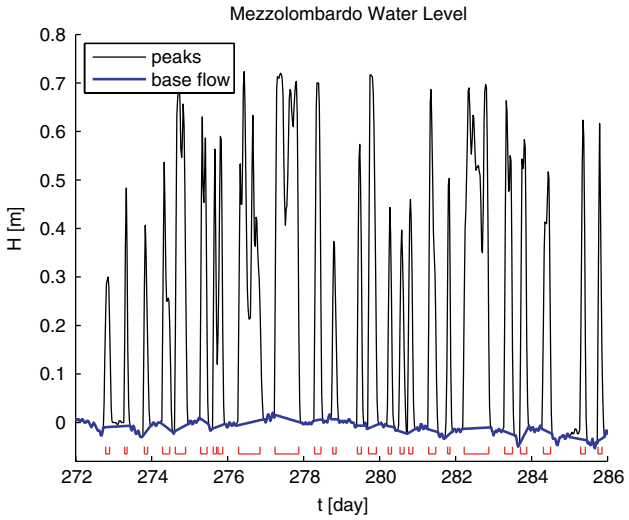

Figure 3. Water level series downstream of Mezzocorona power plant from day 272 (Sunday, 30th September 2007) to day 286 (Sunday, 14th October 2007): an irregular pattern with short period peaks. The duration of the peaking events is visualized through the red segments close to the horizontal axis.

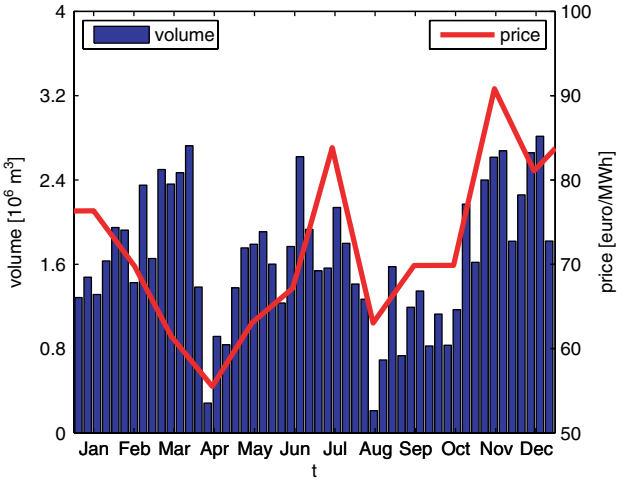

Figure 4. Comparison between the *weekly averaged daily volume of released water from the Mezzocorona power plant (in* $10^6 m^3$ *units)* and the monthly averaged price of energy (Italian official price, €/*MWh*; source: elaboration of the National Authority for Electric Energy and Gas, based on the data by GME, http://www.autorita.energia.it/it/dati/eep40.html (accessed 22 October 2009).

where Q is the discharge measured in m^3/s and $a = 56{\cdot}14\ m^{3-c}/s$, $b = 0{\cdot}31$ m, $c = 1{\cdot}92$. An example of the water level measured in summer 2007 is shown in Figure 2. A typical scenario with no hydropeaking during Sundays (days 188 and 195) and Saturday afternoon (day 194) clearly appears. This is associated with a rather predictable pattern of hydropower production occurring during the whole day from Monday to Friday, which may split into two separate segments, like for day 191, or reduce around noon, like for days 190, 192 and 193. Disentangling single events is not always straightforward, because the individuation of two daily peaks depends on the assumed thresholds (cf., for instance days 191 and 193), as discussed in Section on Threshold Analysis.

The characteristics of hydropeaking events change during the year. In some periods, the water is released every day of the week at the maximum rate; in other periods (see, for instance Figure 3), the requests of the energy market determine a more irregular pattern of hydropower production that causes short-period, irregular water level peaks. The relationship between hydropeaking and the price of energy can be easily argued by looking at Figure 4, where the weekly averaged daily volumes of released water are compared with the monthly averaged energy prices, referred to the central day of each month. The plot clearly shows that hydroelectricity production is reduced when the average price diminishes (April and August), although an even closer correlation can be expected if maximum instead of averaged prices are used. Although referring to average figures, the seasonal trend emerging from Figure 4 parallels that associated with intra-annual variations in the intensity and frequency of the peaking events, which will be examined in more detail in Section on Seasonal Variations in the Thermopeaking Effects.

Figure 5 summarizes the behaviour of two key characteristics of the hydropeaking events along the year: the events duration Δt and their intensity ΔH, defined as the maximum water level jump relative to the base flow. Multiple events have been accounted for separately. Figure 5 provides an overall indication of those periods during the year that have been characterized by a reduction in intensity (and frequency) of the events, which can also be associated with the reduced electricity production shown in Figure 4. Cumulative distributions of event durations and of maximum hydropeaking jumps are reported in Figure 6a and b, respectively, on the basis of time classes of 1 h. Both primary hydropeaking events, as single events, and separate multiple events have been considered.

The main result is that the distribution of duration is bimodal, with one peak at about 6–8 h and another one around 18 h for single events (Figure 6c). The distribution is also approximately bimodal considering multiple events, whose number is about 10% larger than single events (Figure 6d). In this case, the peaks are shifted towards shorter durations: the former peak is around 3–6 h, the latter on 15 h. The two peaks can be recognized as characteristics of two typical hydropower generation schemes: half-day production occurring in the morning or in the afternoon only and the whole day production, continuously occurring from morning to evening.

Thermopeaking characterization

Distinguishing the thermal alterations caused by the hydropower releases from the diurnal cycle due to the variation in the net external energy input is not an obvious task if only one gauging station is considered. In particular, it is more complex than individuating hydropeaking events, for which the basic flow usually varies on a longer time scale, and hence it is relatively easy to separate the two contributions, although this may not be the case for rivers subjected to glacial melting with strong diurnal

Copyright © 2010 John Wiley & Sons, Ltd.

DOI: 10.1002/eco

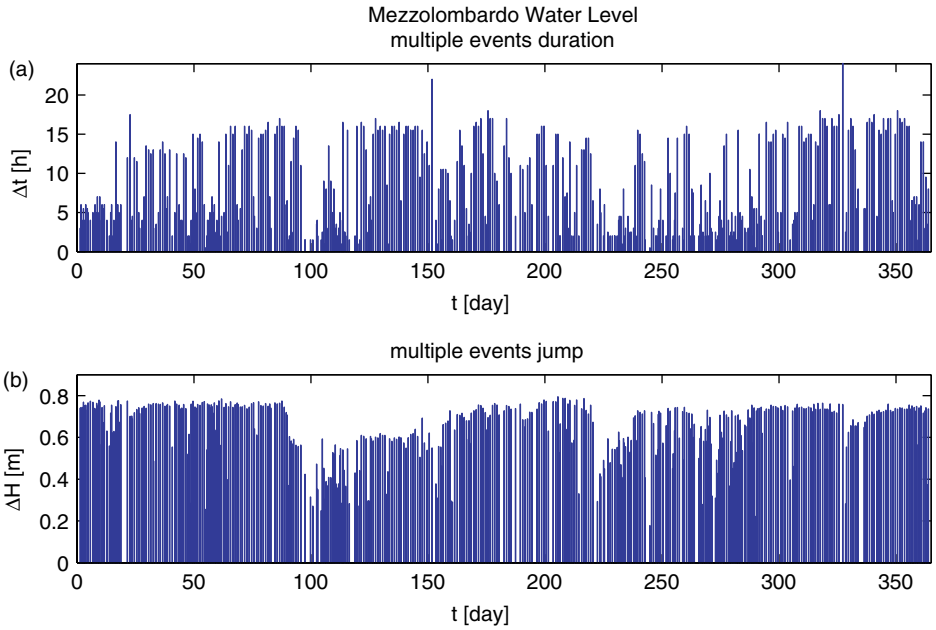

Figure 5. Characteristics of hydropeaking events in Mezzolombardo during 2007 (considering multiple events): (a) event duration Δt; (b) event peak value ΔH.

streamflow variations. As a rule, a reliable characterization of thermopeaking requires information from two gauging stations, located upstream and downstream of the hydropower release. Applying a suitable time shift to one of the two records allows comparing the upstream and downstream temperature signals, and hence to obtain the net amount of thermal alteration ΔT by subtraction. The value of the time shift depends on the mean flow velocity and it can also be determined examining the covariation between the two signals.

We refer to the case of the Mezzocorona power plant release in order to investigate in detail the properties of thermopeaking. Owing to the distance between the thermal gauging stations (see Figure 1), the convective shift among the upstream and downstream series is approximately 0·05 day (1·2 h).

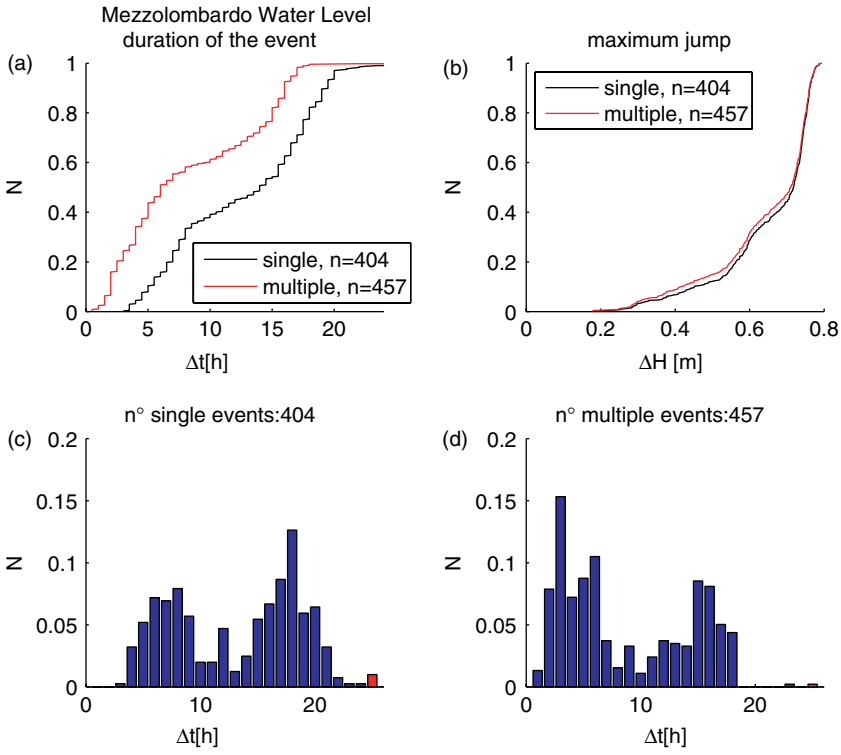

Figure 6. Main characteristics of the hydropeaking events in Mezzolombardo (year 2007): (a) cumulative frequency, normalized as $N = n/n_{tot}$, of the event duration Δt (subdivided in classes of 1 h); (b) cumulative frequency of the event peak value ΔH; (c) frequency distribution of the event duration Δt; (d) same as (c) but considering separate multiple events. The red bar at 25 h indicates the sum of the events with duration longer than 1 day.

Copyright © 2010 John Wiley & Sons, Ltd.

DOI: 10.1002/eco

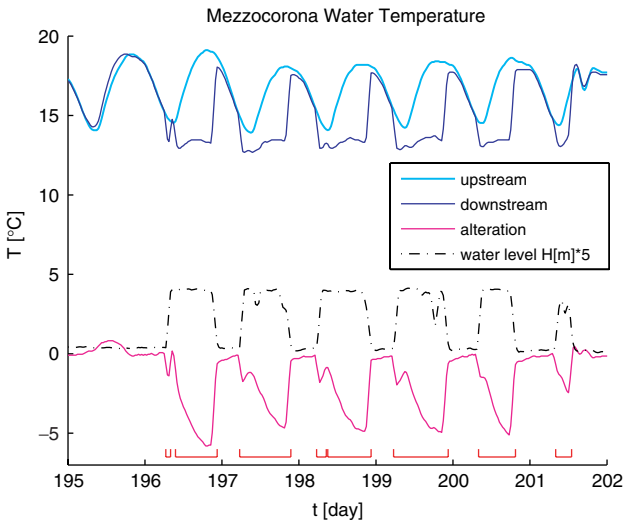

Figure 7. Water temperature upstream (thick cyan line) and downstream (blue line) Mezzocorona hydropower release from day 195 (Sunday, 15th July 2007) to day 202 (Sunday, 22nd July 2007). The temperature difference (magenta line) individuates cold thermopeaking events, which are consistent with hydropeaking events (dash-dot black line) as described by the strong water level fluctuations (H is shown on the temperature axis in meters multiplied by 5 °C/m). The duration of the cold thermopeaking events is visualized through the red segments close to the horizontal axis.

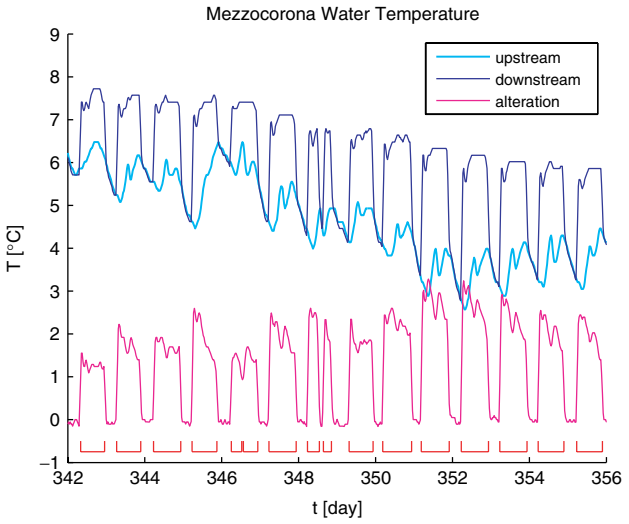

Figure 8. Water temperature upstream (thick cyan line) and downstream (blue line) of Mezzocorona hydropower release from day 342 (Sunday, 9th December 2007) to day 356 (Sunday, 23rd December 2007). The temperature difference (magenta line) individuates warm thermopeaking events, whose duration is visualized through the red segments close to the horizontal axis.

Figure 7 shows how the thermally altered streamflow affects the daily temperature cycle. In the period considered (1 week in July), the water temperature in the reservoir is lower than that of the receiving stream: hence what can be defined a *cold thermopeaking* occurs. The duration of the thermopeaking events is compared with the ones estimated by means of water level variations (dash-dot line), showing a noticeable agreement. It is worth noting that the magnitude of the thermal alteration (up to 6 °C in this case) is comparable with the sinusoidal diurnal variation in the undisturbed upstream reach (approximately 5 °C).

In fact, a simple energy balance holds,

$$Q_u T_u + Q_r T_r = Q_d T_d \tag{8}$$

where Q is the discharge, T is the temperature, and subscripts refer to the upstream reach (u), hydropower release (r) and downstream reach (d), where $Q_d = Q_u + Q_r$ at the confluence. The equality is only approximate because the external energy inputs are neglected in the balance, which assumes an instantaneous mixing process. The temperature after mixing is then

$$T_d = T_r - \frac{Q_u}{Q_r}(T_d - T_u) \tag{9}$$

Considering some reference values of the variables during the altered period ($Q_u = 8$ m^3/s, $Q_d = 68$ m^3/s, $Q_r = 60$m^3/s, $T_u = 19$ °C, $T_d = 13$ °C), it follows that $T_d \simeq T_r + 0{\cdot}8$ °C and hence the reservoir temperature can be estimated approximately as $T_r \sim 12$ °C. Therefore, because the released discharge is much larger than the upstream discharge ($Q_u/Q_r \ll 1$) and the temperature in the downstream reach is almost coincident with T_r, T_d keeps constant during the period of hydropower production, as it appears in Figure 7.

An opposite behaviour is shown during the winter season, where a *warm thermopeaking* occurs due to the higher temperature of reservoir water (in particular, for withdrawal of hypolimnetic water if the reservoir may be considered as partially stratified) with respect to the river temperature. This is illustrated in Figure 8, where two weeks of regular hydropeaking are considered. In this case, the thermal alteration (up to 3 °C) is notably larger than the natural daily variation (approximately 1 °C).

The beginning and end times of thermopeaking events are relatively constant: roughly, from morning to evening for the whole day production if considering a river reach close to the hydropower release. Therefore, it is easy to understand the different behaviour of the cold and warm thermopeaking. In fact, in the former case (Figure 7), the river temperature is reduced when the natural heating would increase. If thermopeaking is long enough, water temperature may not be affected by the diurnal cycle and remain almost constant during day and night (this does not occur in the Mezzocorona because there is an abrupt temperature increase at late evening when hydropower production ends). In the opposite case (warm thermopeaking, Figure 8), the temperature is artificially increased in correspondence with the beginning of the natural daily cycle (reduced during winter). As a consequence, the daily excursion of temperature is significantly increased.

A more general picture can be drawn considering the whole year 2007 (Figure 9). The alterations of the temperature give rise to an annual cycle of warm and cold thermopeaking, having two opposite maxima in November, when the reservoir is still warmer than the river, and in May, when the reservoir has not been affected by the summer heating yet. In order to clarify

Copyright © 2010 John Wiley & Sons, Ltd.

DOI: 10.1002/eco

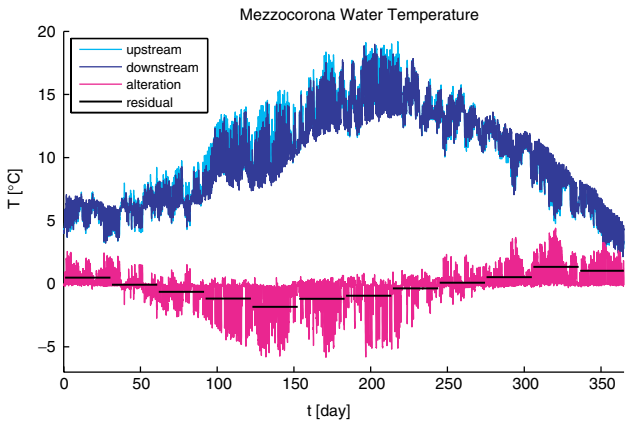

Figure 9. Water temperature at Mezzocorona gauging stations during year 2007: upstream (cyan), downstream (blue) temperatures, instantaneous alterations (magenta), and monthly residual variation (black segments).

the cumulative effect of such alterations, we introduce the integral of the temperature alterations

$$\mathcal{D}(t_1;t_2) = \int_{t_1}^{t_2} \Delta T(\widehat{t})\mathrm{d}\widehat{t} \tag{10}$$

which expresses the differences in terms of degree days between the two sections, and the average effect over the period

$$\Delta T_a = \frac{\mathcal{D}(t_1;t_2)}{t_2 - t_1} \tag{11}$$

The monthly (i.e. $t_2 - t_1 \simeq 30{\cdot}5$ days) residual variations are shown in Figure 9 by means of black segments. They indicate the average variation of temperature perceived by the ecosystem during the period. Cold thermopeaking months in the Noce River in 2007 occur from March to July, and warm thermopeaking from September to January, with August and February being transitional months. Although our record refers to year 2007, such seasonality is likely to exhibit little variations from year to year.

Impact of thermopeaking at different scales

In order to analyse the thermal alteration at different time scales, we apply the WT analysis to the 30-min temperature dataset. Upstream/downstream differences in the Wavelet Power Spectra (WPS) allow to detect the most affected time scales. Note that hereafter the terms 'scale' and 'period' will be used with the same meaning, because they are nearly equivalent for the Morlet wavelet that has been chosen as mother wavelet in the present analysis. In this respect, it can be interesting to compare an artificial channel junction, resulting from the lateral input of released water, with a more natural configuration, where a hydropower-free lateral tributary with comparable discharge magnitudes joins the main river channel. Such reference junction is provided in the Noce River basin by the Rabbies-Noce confluence, located in the middle part of the basin at an altitude of nearly 900 m asl (see Figure 1 and Section on Materials and Methods).

The panels (a and d) of Figure 10 show the river water temperature 2007 time series recorded immediately upstream and downstream the inlet from the Mezzocorona power plant. Panels (b and e) show the corresponding WPS while the GWS is reported in panels (c and f). The WPS together with the GWS illustrate global and local properties of the signal energy expressed in terms of thermal oscillations. The yellow band (locally turning to red) at the scale of 1 day reflects the diel thermal fluctuations in both the upstream and downstream temperature series. The corresponding peak appearing on the respective GWSs (Figure 10c and f) confirms that the diel scale is one of the most significant in the thermal regime: it does not seem to be much affected by the hydropeaking release in the average. Some energy is also associated to shorter periods of oscillations, but yellow (i.e. more energetic) spots in Figure 10b and e are more irregularly distributed over time, with more evident upstream/downstream differences in comparison to the daily period. The weekly scale is another relevant oscillation period displaying discrepancies between the upstream and downstream temperature series, at least when time-averaging over the whole year. Furthermore, the signal energy grows faster when moving towards larger oscillation periods due to the seasonal fluctuation that, however, cannot be correctly captured by the present analysis.

Figure 11 shows the ratio ρ_{GWS} between the GWS of the upstream and downstream temperature series at the hydropower-impacted Mezzocorona junction (continuous line) and at the Rabbies junction (dashed line). Unit values of ρ_{GWS} indicate the absence of time-averaged alteration at that period of oscillation. Therefore, periods with values of ρ_{GWS} that differ significantly from unity are the most thermally impacted by the junction. The strongest relative thermal alteration in the artificial (Mezzocorona) junction is associated with the sub-daily scales, where the downstream time-averaged energy is more than four times larger with respect to the upstream temperature series. In contrast, the oscillations at the daily scale is slightly reduced (~20%), while thermopeaking might increase up to 50% the energy of thermal oscillation at larger scales. In particular, the weekly scale might reflect a residual tendency to reduce hydropower production during weekends.

Comparing the downstream thermal alteration between the two types of junctions, we must keep in mind that these alteration relate to two main effects. One is the temperature difference between the upstream channel and the lateral release, while the other is the hydropeaking intensity, defined in terms of the streamflow ratio between the same channels. Both parameters are strongly time-dependent at various scales and the available dataset does not allow a close separation between them, particularly in the case of the Rabbies junction.

The strong thermal alteration occurring at short scales confirms the importance of examining short-term events

Copyright © 2010 John Wiley & Sons, Ltd.

DOI: 10.1002/eco

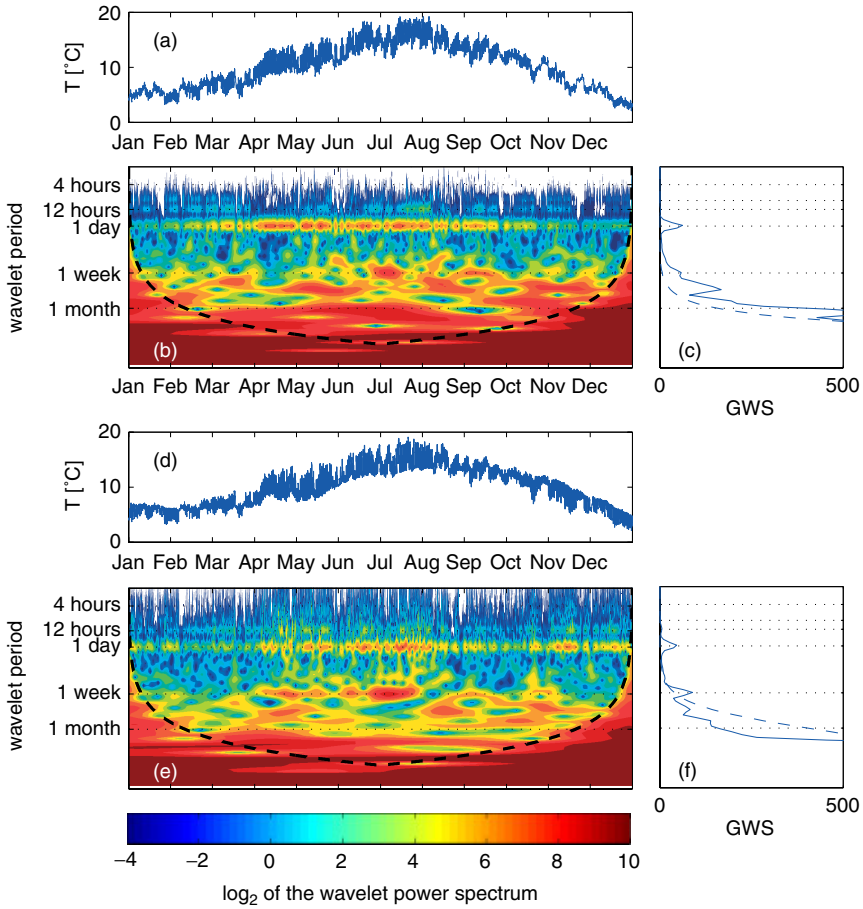

Figure 10. Results of the WT applied to the water temperature series measured immediately upstream (a-c) and downstream (d-f) the release from the Mezzocorona power plant. (a and d) Temperature time series; (b and e) Wavelet Power Spectra; (c and f) Global Wavelet Spectra.

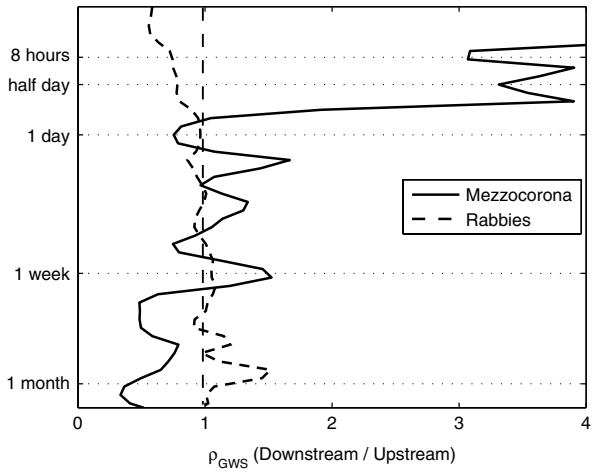

Figure 11. Ratio ρ_{GWS} between the downstream and upstream GWS of the Mezzocorona and Rabbies confluences. A unit ratio indicates in the average absence of thermal alteration downstream of the confluence on a yearly basis..

in order to build a complete picture of hydropower-related thermal alteration. Figure 6 indicates a characteristic bimodal distribution of the hydropeaking event duration. One peak relates to sub-daily scales, and may range from 5 to 8 h, depending on how the presence of multiple events is accounted for when counting the events. The second peak corresponds to much longer releases, which mainly last from 15 to 17 h. The strong alteration at sub-daily scales emerging from Figure 11, in the case of the Mezzocorona junction, is therefore likely due to the short-lasting peaking events, while the average impact of longer lasting releases seems to produce a relatively weaker effect. This can be detected in Figure 11 for some of the periods longer than 1 day, with maximum downstream alterations up to 1·5 times with respect to the upstream signal.

Overall, the application of WT analysis shows that the sub-daily time scales are those most affected by thermopeaking, thus confirming the need of high time-resolution datasets to completely characterize the thermal regime in river catchments where hydropower production occurs. Moreover, beyond yearly averaged differences that can be observed at different time scales, it is evident from the spectra in Figure 10 that the upstream/downstream comparison yields different results in different times of the year with potential severe ecological effects. These seasonal variations are examined in more detail in the next subsection.

Seasonal variations in the thermopeaking effects

The Scale-Averaged Wavelet Power is a useful indicator to investigate in more detail how the effects of thermal alteration at a given time scale change during the year.

Copyright © 2010 John Wiley & Sons, Ltd.

DOI: 10.1002/eco

The SAWP is indeed a measure of the signal variability at a given period of oscillation: it can be thought as measure of the *local* standard deviation of the temperature series at the scale of interest, which varies with time. Figure 12 shows the SAWP computed at the daily scale for the Mezzocorona and for the Rabbies junctions. Values have been made dimensional through the standard deviation of each series. In the near-natural Rabbies junction (Figure 12a), upstream daily temperature oscillations are essentially unmodified by the lateral input of the Rabbies stream. In winter time, diel temperature oscillates of nearly 1 °C, while the fluctuation range extends up to 7 °C in the warmest months. Despite the streamflow of the Rabbies Creek is often comparable to that of the receiving Noce River, thermal differences between the two streams are not high enough for significant heat exchanges to occur. On the contrary, Figure 12b indicates that thermopeaking associated to the Mezzocorona power plant is able to substantially modify the daily thermal oscillations occurring upstream (blue line) of the release. The downstream (red line) daily thermal oscillations are indeed damped up to 3–4 °C in April and May, a trend which persists in early summer months. In contrast, in November and December due to hydropeaking, the Noce River can experience diel fluctuations of 4–5 °C compared with an average of 1 °C occurring in the section upstream of the release.

Differences Δ_{SAWP} between downstream and upstream SAWPs can be used to examine alterations of the thermal oscillations at any time scale of interest. In addition to the daily scale of oscillation, it is interesting to focus also on the strongly altered sub-daily scales (see Figure 11) and on the weekly scale. Figure 13 quantifies downstream–upstream SAWP differences (Δ_{SAWP}) for the Mezzocorona junction at the 8-h, daily and weekly scale in the form of box-and-whiskers plots. The quartiles and ranges have been computed on the values of Δ_{SAWP} series for each month separately, in order to immediately highlight seasonal variations. Figure 13b is therefore a different representation of the same information contained in Figure 12b for the daily scale of oscillation: it shows that the monthly mean amplitude of thermal oscillations is reduced from February to September and is enhanced from November to January. Figure 13a and c shows different trends occurring at sub-daily and weekly scales. At the 8-h scale, short-term temperature oscillations can be increased by thermopeaking events up to 2–3 °C from April to August and, albeit to a lower extent (1–1·5 °C), also from October to January. This is likely associated with events corresponding to the first peak in Figure 6 and can be detected thanks to the relatively high sampling interval of the collected dataset, which is several times smaller than the averaged duration of the shortest events. The monthly mean SAWP alteration related to these short-term events is lower (up to

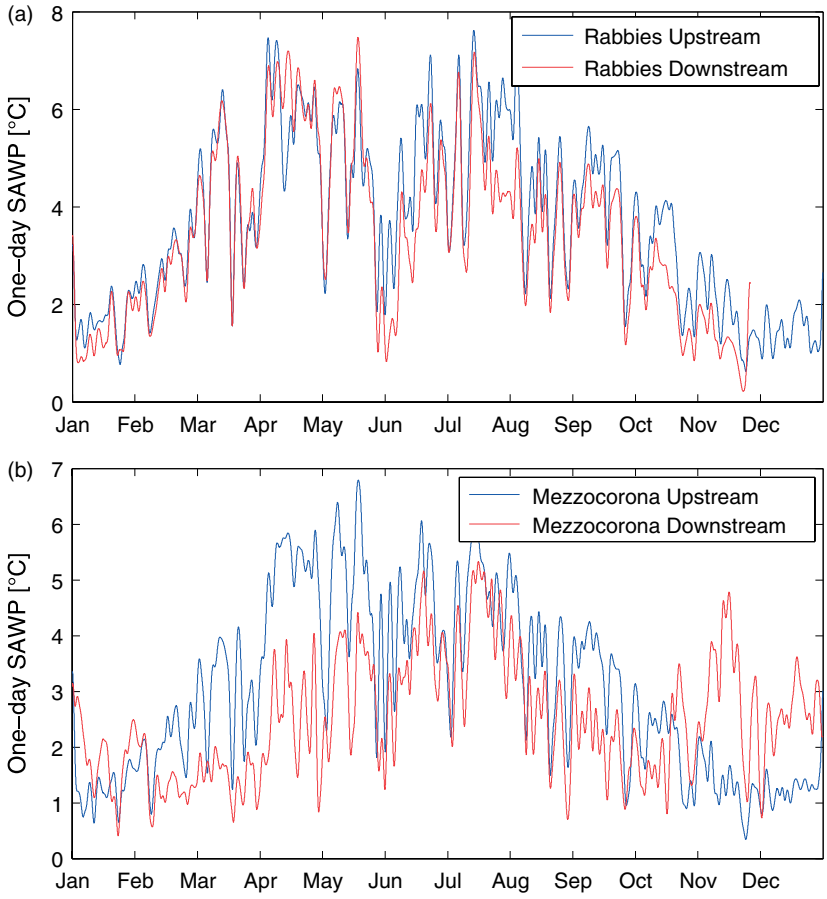

Figure 12. One-day SAWP for temperature series upstream (blue line) and downstream (red line) the Rabbies (a) and the Mezzocorona (b) junctions.

Copyright © 2010 John Wiley & Sons, Ltd.

DOI: 10.1002/eco

1 °C) with respect to that occurring at the daily scale (cf. Figure 13a and b): this notwithstanding, the large number of outliers in Figure 13a suggests the repeated, irregular occurrence of stronger localized alterations (2–3 °C) also at this scale, which may also have severe ecological consequences. This also indicates the importance of focussing on these sub-daily scales of oscillation to avoid the loss of possibly ecologically relevant information.

The behaviour of the difference Δ_{SAWP} at the week scale parallels that at the 8-h period from April to July, whereas weekly oscillations follow a more irregular trend in fall months and are reduced by thermopeaking in winter times. Maximum alterations at the week scale, however, keep more confined with respect to other scales, being almost invariably lower than 1 °C.

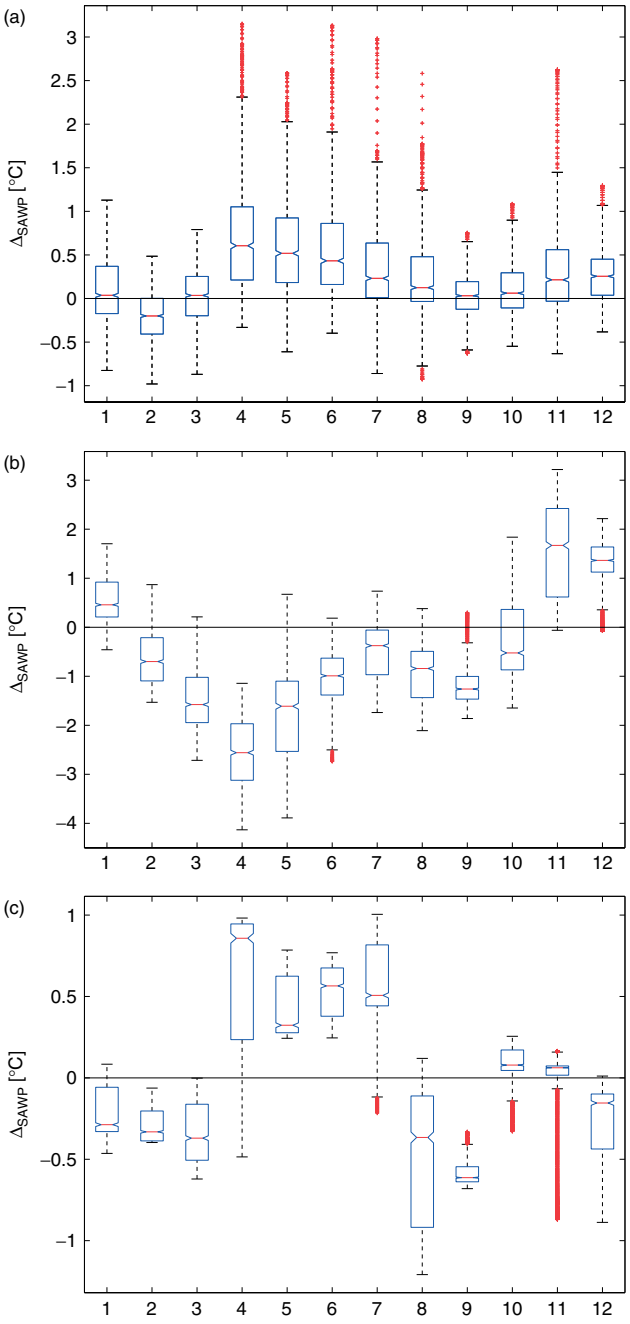

Figure 13. Box-and-whiskers plot of the difference Δ_{SAWP} between the downstream and upstream Scale-Averaged Wavelet Power of the temperature series at the Mezzocorona junction for periods of 8 h (a), 1 day (b) and 1 week (c).

The seasonality that can be observed in the comparison between upstream and downstream SAWPs at the daily scale parallels that associated with the succession of warm and cold thermopeaking events (Figure 9). It has been noted in Section on Thermopeaking Characterization that warm thermopeaking causes an additional heating with respect to what would occur naturally from approximately October to February. This results in downstream amplification of the thermal oscillations and therefore can be associated with the positive values of Δ_{SAWP} appearing in Figure 13a and b during the winter months. In contrast, cold thermopeaking, occurring approximately from April to August (Figure 9), results in cooling down the river water that would be naturally heated by external exchanges. This reduces the thermal oscillations in the downstream section, thus implying negative values of Δ_{SAWP} that can be observed in the same months at the daily scale (Figure 13b).

The analysis of upstream–downstream differences among the Scale Averaged Wavelet Power at sub-daily, daily and weekly scales therefore allows to quantify the seasonalities associated with thermopeaking effects at these scales. Upstream–downstream variations in the thermal fluctuations are stronger at the 8-h and at the daily scale, and result in opposite trends during summer months, while they are both associated with increased thermal oscillations during winter months.

DISCUSSION AND CONCLUSIONS

The present study provides a detailed quantification of the short-term alteration of the thermal regime in the Noce River, a typical hydropower-regulated Alpine stream. Besides representing the first study related to the river thermal regime alteration in a Italian Alpine basin, it allows a better quantitative understanding of the complexity associated with water temperature regimes in regulated streams, particularly at the short time scales affected by hydropower production. The outcomes of the analysis indicate a series of previously unknown thermal effects at multiple scales which might strongly affect biological communities in similar geographical and regulation contexts. Indeed strong biological alterations have been documented (Bruno *et al.*, 2009) in the same Noce River downstream of the Cogolo power station (see Figure 1), where strong hydropeaking and thermopeaking occur. It is therefore reasonable to hypothesize that the river biota may also be severely affected by thermopeaking further downstream under analogous regulation effects.

In analogy with *hydropeaking*, we propose the terminology *thermopeaking* to denote the sharp temperature variations associated with the sudden instream water releases downstream of the power plants. In order to quantify thermal alterations related to hydropeaking, we have first devised a suitable event-detection method based

Copyright © 2010 John Wiley & Sons, Ltd.

DOI: 10.1002/eco

on the time derivative of the data series in order to define which records, within the temperature series, belong to the events. This can be properly achieved referring to the water level series, where sharp temporal variations invariably occur all year-round, allowing to precisely detect beginning and end times. On the contrary, automated event detection on the temperature series would be much difficult, because temperature variations in time may not be always be sharp enough. This is related to the interplay between the heat fluxes associated with river–atmosphere exchanges and with hydropeaking releases, which produces different effects on the temperature series, depending on the time of the release during the day, and varies across different seasons. In the Noce River, the rising and falling of hydro- and thermopeaking are comparable with the period of the sampling interval (nearly 30 min), and events might have two typical durations, in the ranges between 5–8 and 15–18 h. The time distribution of thermopeaking reflects the pattern of hydropower production driven by price fluctuations in the energy market and thus often deviates from the fairly regular pattern consisting of energy production during daytime in the working days, which was typical in the Alps until the past decade.

Warm thermopeaking occurs from September to January and results in additional (up to 4 °C) heating with respect to that associated with the natural diel fluctuations. On the contrary, *cold* thermopeaking occurs from March to July and cools down the temperature (up to 6 °C), in contrast with the natural trend that would result in heating during the day. As a consequence, temperature temporal oscillations recorded downstream of the release are amplified in the average during winter compared with summer season. Overall, the key differences between natural and man-made temperature variations that can be drawn from the present study are as follows: rates of temperature changes are much faster (see Figures 7 and 8) and contrasting seasonal effects are associated with repeated thermopeaks (Figure 12).

The application of Wavelet Transform (WT) allows to identify how this succession of events affects the thermal river regime at various time scales, from those of a few hours to weekly thermal oscillations. Application of WT to study short-term temperature alterations due to dam regulation has been proposed by Steel and Lange (2007) on several daily temperature series in the Willamette River Basin (USA), regulated by a series of large, multipurpose dams. Although it can be expected that the difference in dam purposes might determine different type of thermal alterations, it is worth attempting a comparison between the outcomes of the two analysis. Steel and Lange (2007) found reductions in water temperature variability, defined as the variability of the wavelet coefficients, as a result of dam regulation at the 1-, 2-, 4- and 8-day scales. No significant differences have been detected in water temperature variability between managed and natural flows at the 16- and 32-day scale. The outcomes of our study confirms that the strongest variability applies for the smaller scales, with a strong increase in temperature variability at sub-daily scales, which could not be detected by Steel and Lange (2007). The present analysis shows that such time-averaged figures are also subject to marked seasonal variations at the sub-daily, daily and weekly scales, with potentially relevant ecological effects.

The quantification of thermopeaking events and of their thermal effects at multiple time scales suggests that hydropower regulation have significantly muted the small time scale variability in temperature patterns to which many organisms may have adapted. Conserving or restoring natural temperature patterns in rivers will require attention to these small-scale thermal alterations and to their potential ecological consequences. This reinforces the need, already raised by Brown and Hannah (2008), of better identifying dynamics and dominant factors/processes operating at different space and timescales, and to underpin accurate prediction of thermal impacts of climate and human-induced change. The complexity of temperature variability at small space scales has been documented in undisturbed rivers (Cardenas *et al.*, 2008; Acuna and Tockner, 2009). To the best of our knowledge, yet, no research has examined the ecological effects of the frequent and intermittent changes associated with thermopeaking that occur downstream of hydropower plants at short time scales (daily and sub-daily) on the riverine biota and bio-chemical processes. Experimental research is therefore needed to assess how thermopeaking is likely to influence phases such as larval growth rates, adult emergence or behavioural drift, this appears of specific relevance to complement many studies that highlighted the importance of river thermal regimes as drivers of ecological processes and of aquatic communities dynamics at much longer scales (Ward and Stanford, 1979).

ACKNOWLEDGEMENTS

This work has received financial support from the REPORT project, funded by the Adige River Basin Authority and from the INTERREG-IVB ALPINE SPACE 'ALP-WATER-SCARCE' project. The contribution of Mauro Carolli and Martino Salvaro in data collection is gratefully acknowledged.

REFERENCES

Acuna V, Tockner K. 2009. Surface-subsurface water exchange rates along alluvial river reaches control the thermal patterns in an Alpine river network. *Freshwater Biology* **54**(2): 306–320. ISSN 0046–5070. DOI: 10.1111/j.1365–2427.2008.02109.x.

Blanch S, Ganf G, Walker K. 1999. Tolerance of riverine plants to flooding and exposure indicated by water regime. *Regulated Rivers-Research and Management*, **15**(1–3): 43–62. ISSN 0886–9375.

Brown L, Hannah D. 2008. Spatial heterogeneity of water temperature across an alpine river basin. *Hydrological Processes* **22**(7): 954–967. ISSN 0885–6087. DOI: 10.1002/hyp.6982.

Bruno M, Maiolini B, Carolli M, Silveri L. 2009. Short time-scale impact of hydropeaking on hyporheic invertebrates in an Alpine stream (Trentino, Italy). *Annales de Limnologie-International Journal of Limnology* **45**(3): 157–170. ISSN 0003–4088. DOI: 10.1051/limn/2009018.

Bunn SE, Arthington AH. 2002. Basic principles and ecological consequences of altered flow regimes for aquatic biodiversity. *Environmental Management* **30**(4): 492–507.

Copyright © 2010 John Wiley & Sons, Ltd.

Burkholder B, Grant G, Haggerty R, Khangaonkar T, Wampler P. 2008. Influence of hyporheic flow and geomorphology on temperature of a large, gravel-bed river, Clackamas River, Oregon, USA. *Hydrological Processes* **22**(7): 941–953. ISSN 0885–6087. DOI: 10.1002/hyp.6984.

Caissie D. 2006. The thermal regime of rivers: a review. *Freshwater Biology* **51**: 1389–1406.

Cardenas M, Harvey J, Packman A, Scott D. 2008. Ground-based thermography of fluvial systems at low and high discharge reveals potential complex thermal heterogeneity driven by flow variation and bioroughness. *Hydrological Processes* **22**(7): 980–986. ISSN 0885–6087. DOI: 10.1002/hyp.6932.

Cereghino R, Lavandier P. 1998. Influence of hypolimnetic hydropeaking on the distribution and population dynamics of Ephemeroptera in a mountain stream. *Freshwater Biology* **40**(2): 385–399. ISSN 0046–5070.

Daubechies I. 1992. *Ten Lectures on Wavelets*. Society for Industrial and Applied Mathematics: Philadelphia (USA); 357 pp.

Edison. Polo 1 - Noce. Scheda dell'Asta idroelettrica del Noce tra i comuni di revò (tn) e mezzocorona (tn). impianti idroelettrici Taio-Santa Giustina, Mezzocorona. Aggiornamento delle informazioni anno 2007 (in Italian). Technical report, Bolzano (Italy). 2008. Available at http://www.edison.it/edison/site/it/csr/environment/EMAS-papers/idroelettrico.html. 18 June 2008.

Flodmark L, Vollestad L, Forseth T. 2004. Performance of juvenile brown trout exposed to fluctuating water level and temperature. *Journal of Fish Biology* **65**(2): 460–470. ISSN 0022–1112. DOI: 10.1111/j.1095–8649.2004.00463.x.

Foufoula-Georgiou E, Kumar P. *Wavelets in Geophysics*. Academic Press: San Diego, CA (USA); 1995.

Foulger T, Petts G. 1984. Water quality implications of artificial flow fluctuations in regulated rivers. *The Science of the Total Environment* **37**: 177–185.

Frutiger A. 2004. Ecological impacts of hydroelectric power production on the River Ticino. Part 1: thermal effects. *Archiv fur Hydrobiologie* **159**(1): 43–56. ISSN 0003–9136. DOI: 10.1127/0003-9136/2004/0159-0043.

Gore J, Petts J. 1989. *Alternatives in Regulated River Management*. CRC Press: FL. Boca Rato, Florida, USA.

Grubbs S, Taylor J. 2004. The influence of flow impoundment and river regulation on the distribution of riverine macroinvertebrates at Mammoth Cave National Park, Kentucky, USA. *Hydrobiologia* **520**(1–3): 19–28. ISSN 0018–8158.

Hannah D, Webb B, Nobilis F. 2008. River and stream temperature: dynamics, processes, models and implications - Preface. *Hydrological Processes* **22**(7): 899–901. ISSN 0885–6087. DOI: 10.1002/hyp.6997.

Holland S, Mansur E. 2008. Is real-time pricing green? The environmental impacts of electricity demand variance. *Review of Economics and Statistics* **90**(3): 550–561. ISSN 0034–6535.

Jansson R, Nilsson C, Dynesius M, Andersson E. 2000. Effects of river regulation on river-margin vegetation: a comparison of eight boreal rivers. *Ecological Applications* **10**(1): 203–224. ISSN 1051-0761.

Kaiser G. 1994. *A Friendly Guide to Wavelets*. Birkhäuser: Boston (USA).

Katul G, Schieldge J, Hsieh C, Vidakovic B. 1998. Skin temperature perturbations induced by surface layer turbulence above a grass surface. *Water Resources Research* **34**(5): 1265–1274. ISSN 0043–1397.

Kumar P, Foufola-Georgiou E. 1993. A multicomponent decomposition of spatial rainfall fields. 1. Segregation of large-scale and small-scale features using Wavelet transforms. *Water Resources Research* **29**(8): 2515–2532. ISSN 0043–1397.

Lau KM, Weng H. 1995. Climate signal detection using wavelet transform: how to make a time series sing. *Bulletin of the American Meteorological Society* **76**(12): 2391–2402. ISSN 0003–0007.

Montgomery D, Beamer E, Pess G, Quinn T. 1999. Channel type and salmonid spawning distribution and abundance. *Canadian Journal of Fisheries and Aquatic Sciences* **56**(3): 377–387. ISSN 0706-652X.

Nilsson C, Jansson R, Zinko U. 1997. Long-term responses of river-margin vegetation to water-level regulation. *SCIENCE* **276**(5313): 798–800. ISSN 0036–8075.

Rea N, Ganf G. 1994. Water depth changes and biomass allocation in 2 contrasting macrophytes. *Australian Journal of Marine and Freshwater Research* **45**(8): 1459–1468. ISSN 0067–1940.

Sawyer A, Cardenas M, Bomar A, Mackey M. 2009. Impact of dam operations on hyporheic exchange in the riparian zone of a regulated river. *Hydrological Processes* **23**(15): Special Issue: 2129–2137. ISSN 0885–6087. DOI: 10.1002/hyp.7324.

Scruton D, Pennell C, Ollerhead L, Alfredsen K, Stickler M, Harby A, Robertson M, Clarke KD, LeDrew L. 2008. A synopsis of 'hydropeaking' studies on the response of juvenile Atlantic salmon to experimental flow alteration. *Hydrobiologia* **609**: 263–275. ISSN 0018–8158. DOI: 10.1007/s10750-008-9409-x.

Siviglia A, Toro E. 2009. WAF method and splitting procedure for simulating hydro- and thermal-peaking waves in open-channel flows. *Journal of Hydraulic Engineering-ASCE* **135**(8): 651–662. ISSN 0733–9429. DOI: 10.1061/(ASCE)HY.1943–7900.0000054.

Steel E, Lange I. 2007. Using wavelet analysis to detect changes in water temperature regimes at multiple scales: effects of multi-purpose dams in the Willamette River basin. *River Research and Applications* **23**(4): 351–359. ISSN 1535-1459. DOI: 10.1002/rra.985.

Toffolon M, Siviglia A, Zolezzi G. In press. Thermal wave dynamics in rivers affected by hydropeaking. *Water Resources Research* 2009. (submitted) DOI:10.1029/2009WR008234..

Torrence C, Compo GP. 1998. A practical guide to wavelet analysis. *Bulletin of the American Meteorological Society* **79**: 61–78.

Ward J, Stanford J. 1979. Ecological factors controlling stream zoobenthos with emphasis on thermal modifications of regulated streams. *The Ecology of Regulated Streams*. Plenum Press: New York.

Webb B, Hannah D, Moore R, Brown L, Nobilis F. 2008. Recent advances in stream and river temperature research. *Hydrological Processes* **22**(7): 902–918. ISSN 0885–6087. DOI: 10.1002/hyp.6994.

Zolezzi G, Bellin A, Bruno MC, Maiolini B, Siviglia A. 2009. Assessing hydrological alterations at multiple temporal scales: Adige River, Italy. *Water Resour. Res.* **45**: W12421, DOI:10.1029/2008WR007266.

Copyright © 2010 John Wiley & Sons, Ltd.